J|A|C|S
ARTICLES
Published on Web 06/17/2006

Chiral Templating of Surfaces: Adsorption of (*S*)-2-Methylbutanoic Acid on Pt(111) Single-Crystal Surfaces

Ilkeun Lee and Francisco Zaera*

Contribution from the Department of Chemistry, University of California, Riverside, California 92521

Received March 9, 2006; E-mail: zaera@ucr.edu

Abstract: The adsorption and thermal chemistry of (*S*)-(+)-2-methylbutanoic acid ((*S*)-2MBA) on Pt(111) single-crystal surfaces was characterized by using temperature programmed desorption (TPD) and reflection-adsorption infrared (RAIRS) spectroscopies. Particular emphasis was placed on the characterization of the chiral superstructures formed upon the deposition of the submonolayer coverages of enantiopure (*S*)-2-methylbutanoate species that are produced by thermal dehydrogenation of the (*S*)-2MBA. The enantioselectivity of the empty platinum sites left open on those structures were identified by their difference in behavior toward the adsorption of the two enantiomers of propylene oxide. It was found that a significant enhancement in adsorption is possible on surfaces with the same chirality of the probe molecule, specifically that the uptake of (*S*)-propylene oxide is larger than that of (*R*)-propylene oxide on (*S*)-2-methylbutanoate adsorbed layers. This contrasts with the lack of enantioselectivity previously reported for the same adsorbate on Pd(111). Detectable differences in adsorption energetics of (*R*)- vs (*S*)-propylene oxide on the (*S*)-2-methylbutanoate/Pt(111) overlayers were measured but deemed not to be the controlling factor in the enantioselectivity reported in this system.

1. Introduction

The market for single enantiomers amounts to over $150 billion in annual sales and accounts for more than half of the profits of the drug industry worldwide: 9 of the top 10 drugs available in pharmacies today are based on enantiomerically pure chiral compounds.[1,2] Among the several procedures available for the manufacture of enantiomerically pure compounds,[3−7] many rely on catalysis. This is often done with the help of homogeneous catalysts, typically organometallic compounds,[8−10] but metal complexes are expensive, hard to handle, difficult to separate from the products, and poisonous. It would be highly desirable to replace homogeneous systems with safer and cheaper heterogeneous counterparts.

One particularly promising route for the manufacturing of chiral compounds enantioselectively using heterogeneous catalysis is via the hydrogenation of prochiral unsaturated hydrocarbons. Late transition metals such as platinum and palladium are well-known hydrogenation catalysts,[11,12] and although those catalysts are not intrinsically chiral, it has been shown that chirality can be bestowed on them via the adsorption of chiral modifiers.[13] Perhaps the most successful example of this approach has been the modification of platinum and palladium hydrogenation catalysts with chiral cinchona modifiers for the conversion of α-keto esters to α-hydroxo esters.[14−17] In that case it has been suggested that enantioselectivity is induced by the formation of a complex between individual cinchona molecules and the keto reactant to force the hydrogenation selectively on one side of the carbonyl plane.[18,19] The details of the mechanism of this reaction are still far from understood, but recent surface characterization experiments by us[20−24] and others[25,26] have indicated that the performance of the cinchona-modified catalysts is mostly controlled by the characteristics of the adsorption of the individual chiral modifiers.

(1) Caldwell, J. *Hum. Psychopharmacol.* **2001**, *16*, S67.
(2) Rouhi, A. M. *Chem. Eng. News* **2004**, *82*, *No. 24 (June 14)*.
(3) McCague, R.; Smith, A. *Innovations Pharm. Technol.* **1999**, *99*, 100.
(4) Bluhm, L. H.; Wang, Y.; Li, T. *Anal. Chem.* **2000**, *72*, 5201.
(5) Keurentjes, J. T. F.; Voermans, F. J. M. Membrane separations in the production of optically pure compounds. In *Chirality in Industry II: Developments in the Manufacture and Applications of Optically Active Compounds*; Collins, A. N., Sheldrake, G. N., Crosby, J., Eds.; John Wiley & Sons: Chichester, 1997; p 157.
(6) Procter, G. *Asymmetric Synthesis*; Oxford University Press: New York, 1996.
(7) Halgas, J. *Biocatalysts in Organic Synthesis*; Studies in Organic Chemistry Series; Elsevier: Amsterdam, 1992; Vol. 46.
(8) Schmid, R. *Chimia* **1996**, *50*, 110.
(9) Noyori, R. *Angew. Chem., Int. Ed.* **2002**, *41*, 2008.
(10) Knowles, W. S. *Adv. Synth. Catal.* **2003**, *345*, 3.
(11) Rylander, P. N. *Hydrogenation Methods*; Academic Press: London, 1985.
(12) Bond, G. C. *Metal-Catalysed Reactions of Hydrocarbons*; Springer: New York, 2005.
(13) Baiker, A.; Blaser, H. U. Enantioselective Catalysts and Reactions. In *Handbook of Heterogeneous Catalysis*; Ertl, G., Knözinger, H., Weitkamp, J., Eds.; VCH: Weinheim, 1997; Vol. 4; p 2422.
(14) Orito, Y.; Imai, S.; Niwa, S.; Nguyen Gia, H. *Yuki Gosei Kagaku Kyokaishi* **1979**, *37*, 173.
(15) Tungler, A.; Kajtar, M.; Mathe, T.; Toth, G.; Fogassy, E.; Petro, J. *Catal. Today* **1989**, *5*, 159.
(16) Baiker, A. *J. Mol. Catal. A* **1997**, *115*, 473.
(17) Wells, P. B.; Wilkinson, A. G. *Top. Catal.* **1998**, *5*, 39.
(18) Bürgi, T.; Baiker, A. *J. Catal.* **2000**, *194*, 445.
(19) Vayner, G.; Houk, K. N.; Sun, Y.-K. *J. Am. Chem. Soc.* **2004**, *126*, 199.
(20) Kubota, J.; Zaera, F. *J. Am. Chem. Soc.* **2001**, *123*, 11115.
(21) Chu, W.; LeBlanc, R. J.; Williams, C. T.; Kubota, J.; Zaera, F. *J. Phys. Chem. B* **2003**, *107*, 14365.
(22) Ma, Z.; Kubota, J.; Zaera, F. *J. Catal.* **2003**, *219*, 404.
(23) Ma, Z.; Lee, I.; Kubota, J.; Zaera, F. *J. Mol. Catal. A* **2004**, *216*, 199.
(24) Ma, Z.; Zaera, F. *J. Phys. Chem. B* **2005**, *109*, 406.
(25) Burgi, T.; Baiker, A. *Acc. Chem. Res.* **2004**, *37*, 909.
(26) LeBlanc, R. J.; Chu, W.; Williams, C. T. *J. Mol. Catal. A* **2004**, *212*, 277.

10.1021/ja061654w CCC: $33.50

A second successful example of chiral modification in heterogeneous catalysts is that of the enantioselective hydrogenation of β-keto esters on nickel surfaces modified by tartaric acid.[27−29] In this case it is believed that chiral modification is achieved via the formation of ordered suprastructures of the chiral modifier on the surface with chiral void spaces able to selectively adsorb other chiral molecules.[30,31] Ordered structures with chiral empty sites have indeed been identified directly on copper single-crystal surfaces.[32,33] Unfortunately, the results from further work on the more relevant nickel surfaces have been less straightforward to interpret.[34] In separate studies, Tysoe et al.[35] and us[36] have shown an enantiopreference on both Pd(111) and Pt(111) surfaces covered with layers of enantiopure 2-butoxide for the uptake of homochiral propylene oxide molecules. More recently, the Tysoe group have proven that this behavior is quite general, extending to a number of chiral organic acids and amino acids.[37] On the other hand, the Tysoe group have also pointed out that, at least on Pd(111), the extent of the chiral effect seems to vary in a nontrivial manner with the structure of the templating chiral modifier.[37] In particular, their results indicate that templating of the surface with 2-methylbutanoate, which has a similar chiral center than 2-butoxide but anchors to the surface via a carboxylate rather than an alkoxide linkage, leads to no enantiospecificity for the adsorption of enantiopure propylene oxide. They explained their observations by using a model where two anchoring points are required for chiral templating, to avoid free rotation around the main bonding axis and the consequent averaging of the chiral effect. To test that idea and its potential universality on different surfaces, we decided to probe the enantioselective behavior of Pt(111) surfaces templated by such 2-methylbutanoate moieties.

Based on the results of the present study, we question the importance of such a two-point anchoring model in determining the ability of chiral adsorbates to imprint enantioselectivity on the surface and highlight the role that the nature of the metal may play in this chiral templating process. Indeed, our temperature programmed desorption (TPD) and reflection−absorption infrared spectroscopy (RAIRS) data do point to the formation of chiral adsorption sites on Pt(111) by (*S*)-2-methylbutanoate layers, in contrast to the absence of such an effect previously reported on Pd(111). Moreover, the enantioselectivity is manifested here not only by the different amounts of (*R*)- vs (*S*)-propylene oxide that can be adsorbed on a given (*S*)-2-methylbutanoate/Pt(111) layer but also by detectable differences in the energetics of those adsorptions. It is argued here that although the energetic differences are most likely due to individual interactions between the methylbutanoate modifier and the propylene oxide probe, they do not play a predominant role in bestowing enantioselectivity to the surface. Rather, it is believed that it is the formation of chiral suprastructures that still dominates the collective chiral behavior of the modified Pt(111) surface. The arguments for this conclusion are presented below.

2. Experimental Section

All temperature-programmed desorption (TPD) and reflection−absorption infrared spectroscopy (RAIRS) experiments reported here were performed in a two-tier ultrahigh vacuum (UHV) chamber cryopumped to a base pressure below 8×10^{-11} Torr.[38,39] The main stage of this chamber is used for the TPD experiments, which are performed using a computer-controlled quadrupole mass spectrometer (UTI 100C) with an extendible nose cone ended in a 5-mm diameter aperture which can be placed within 1 mm of the single crystal for the detection of molecules desorbing from the front surface of the crystal. A constant heating rate of 10 K/s was used in all TPD runs, and a bias of −100 V was applied to the crystal in order to avoid any chemistry induced by stray electrons from the ionizers of the ion gauge and mass spectrometer.[40] The mass spectrometer is interfaced to a personal computer in order to record the signals of up to 15 different ions during a single TPD experiment.

A second, smaller stage accessible using a long-travel manipulator is employed for the RAIRS experiments. The infrared beam from an FT-IR spectrometer (Bruker Equinox 55) is passed through a polarizer and focused through a NaCl window onto the platinum crystal at grazing (∼85°) incidence. The reflected beam that escapes from the UHV chamber through a second NaCl window is then refocused onto a narrow-band mercury−cadmium−telluride (MCT) detector. The entire beam path is enclosed in a sealed box purged with dry air purified using a scrubber (Balston 75−60) for CO_2 and water removal. All spectra were taken at a resolution of 4 cm^{-1} by averaging over 2000 scans, a process that takes about 4 min per experiment, and ratioed against spectra from the clean surface acquired before gas dosing. Both the condition of the sample and the infrared beam alignment were checked routinely by comparing infrared spectra for a saturation coverage of CO with those reported in the literature.[41,42]

The platinum (111) single crystal, a disk 8 mm in diameter and 2 mm in thickness, was mounted on the sample holder via spot-welding to two tantalum wires attached to corresponding copper electrical feedthroughs. With this arrangement it is possible to cool the sample to below 80 K by using a continuous flow of liquid nitrogen through hollow tubes connected to the nonvacuum side of the copper feedthroughs, and also to heat the crystal resistively to up to 1100 K. The surface temperature is measured with a chromel−alumel thermocouple spot-welded to the side of the crystal and set to within ±1 K of any given value by using a homemade temperature controller also employed to ramp the temperature linearly for the TPD experiments. The sample was regularly cleaned by cycles of oxidation in 5×10^{-7} Torr of oxygen at 700 K and annealing in a vacuum at 1100 K. Ar^+ ion sputtering followed by annealing at 1100 K was used as needed but sparingly to minimize the creation of surface defects.

All the liquid reactants, namely, the (*R*)- and (*S*)-propylene oxide (PO, 99% purity) and the (*S*)-(+)-2-methylbutanoic acid ((S)-2MBA, 98% purity, also known as (*S*)-(+)-methylbutyric acid), were purchased from Aldrich, purified via repeated freeze−pump−thaw vacuum distillations before use, and checked in situ by mass spectrometry. Dosing was achieved by leaking controlled amounts of the vapors into the vacuum chamber, carried out at 80 K unless otherwise indicated, and reported in Langmuirs (1 L ≡ 10^{-6} Torr s), not corrected for differences in ion gauge sensitivities.

(27) Hoek, A.; Sachtler, W. M. H. *J. Catal.* **1979**, *58*, 276.
(28) Izumi, Y. *Adv. Catal.* **1983**, *32*, 215.
(29) Webb, G.; Wells, P. B. *Catal. Today* **1992**, *12*, 319.
(30) Raval, R. *CATTECH* **2001**, *5*, 12.
(31) Humblot, V.; Raval, R. *Appl. Surf. Sci.* **2005**, *241*, 150.
(32) Ortega Lorenzo, M.; Haq, S.; Bertrams, T.; Murray, P.; Raval, R.; Baddeley, C. J. *J. Phys. Chem. B* **1999**, *103*, 10661.
(33) Humblot, V.; Barlow, S. M.; Raval, R. *Prog. Surf. Sci.* **2004**, *76*, 1.
(34) Humblot, V.; Haq, S.; Muryn, C.; Raval, R. *J. Catal.* **2004**, *228*, 130.
(35) Stacchiola, D.; Burkholder, L.; Tysoe, W. T. *J. Am. Chem. Soc.* **2002**, *124*, 8984.
(36) Lee, I.; Zaera, F. *J. Phys. Chem. B* **2005**, *109*, 12920.
(37) Burkholder, L. A.; Stacchiola, D. J.; Tysoe, W. T. Probing chirally templated surfaces. 228th ACS National Meeting, Philadelphia, PA, United States, 2004, COLL-155.
(38) Hoffmann, H.; Griffiths, P. R.; Zaera, F. *Surf. Sci.* **1992**, *262*, 141.
(39) Janssens, T. V. W.; Zaera, F. *J. Catal.* **2002**, *208*, 345.
(40) Zaera, F.; Chrysostomou, D. *Surf. Sci.* **2000**, *457*, 89.
(41) Steininger, H.; Lehwald, S.; Ibach, H. *Surf. Sci.* **1982**, *123*, 264.
(42) Zaera, F. *Surf. Sci.* **1991**, *255*, 280.

Table 1. Vibrational Assignment of the Infrared Spectra of (*S*)-(+)-2-Methylbutanoic Acid (2MBA) Adsorbed on Pt(111)[a]

		5.0 L 2MBA/Pt(111)			1.0 L 2MBA/Pt(111)	
assignment[b]	2MBA liquid[45,46]	100 K	170 K	230 K	100 K	230 K
ν(OH) dimer	3578	3100−3600(br)			3100−3500(br)	
$\nu_a(CH_3)$	2965	2985, 2973	2985, 2971	2988, 2969	2980(br)	2970(sh)
$\nu_a(CH_2)$	2935	2945, 2930	2946, 2932	2946	2950(br)	2950
$\nu_s(CH_3)$	2905	2910	2910	2912	2930	
$\nu_s(CH_2)$	2870	2880	2881	2881	2870	2870
ν(C═O)	1653	1700, 1685(br)	1714	1716, 1700	1620	
$\gamma(CH_2)$	1464	1467	1465	1470	1460(sh)	1470(sh)
$\delta_a(CH_3)$	1439	1456(sh)	1455(sh)	1456	1453	1455
ν(CO) + δ(OH) dimer	1412	1422				
ν_s(OCO) carboxylate				1394		1395
δ(OH)	1386	1385, 1272	1385, 1275			
$\delta_s(CH_3)$		1372, 1360	1358	1368		1365
δ(CH)	1302	1315	1311	1310	1305(br)	1305
ν(CC)	1182	1240, 1230	1238	1215		1220, 1200
$\rho(CH_3)$	1108, 1065	1140, 1093	1140, 1095	1140, 1089		1150
ν(CO) dimer	1024	1018, 983				
$\rho(CH_3)$	974	972	972	967		985
δ_{oop}(OH···O) dimer	914	954				

[a] All frequencies are reported in cm^{-1}. [b] ν = stretching, γ = scissoring, δ = deformation, ρ = rocking, s = symmetric, a = asymmetric, oop = out-of-plane, sh = shoulder, br = broad.

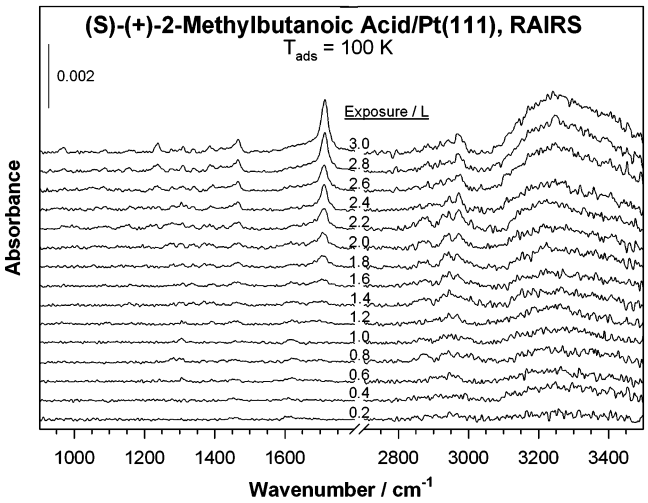

Figure 1. Reflection−absorption infrared spectra (RAIRS) as a function of exposure for (*S*)-(+)-2-methylbutanoic acid ((*S*)-2MBA) adsorbed on a Pt(111) single-crystal surface at 100 K.

3. Results

3.1. Adsorption and Thermal Chemistry of (*S*)-(+)-2-Methylbutanoic Acid. The uptake of (*S*)-(+)-2-methylbutanoic acid ((*S*)-2MBA) on Pt(111) was first characterized at 100 K by RAIRS. The data are reported in Figure 1, and the vibrational assignment given in Table 1.[43,44] The main peaks in the spectra for the condensed multilayers obtained after doses of 2.0 L or more are easily assigned to the carbonyl (ν(C═O), 1714 cm^{-1}) and hydroxo (ν(OH), 3100−3500 cm^{-1}) stretching modes. Also, the broad nature of the latter is easily explained by hydrogen bonding and dimer formation. Other prominent bands include those for the methyl C−H asymmetric stretch ($\nu_a(CH_3)$, 2973 cm^{-1}), methylene scissoring ($\gamma(CH_2)$, 1467 cm^{-1}), methylene deformation ($\delta(CH_2)$, 1385 cm^{-1}), and C−O stretching (ν(CO), 1239 cm^{-1}) modes. These spectra are consistent with those available for the pure liquid.[45,46]

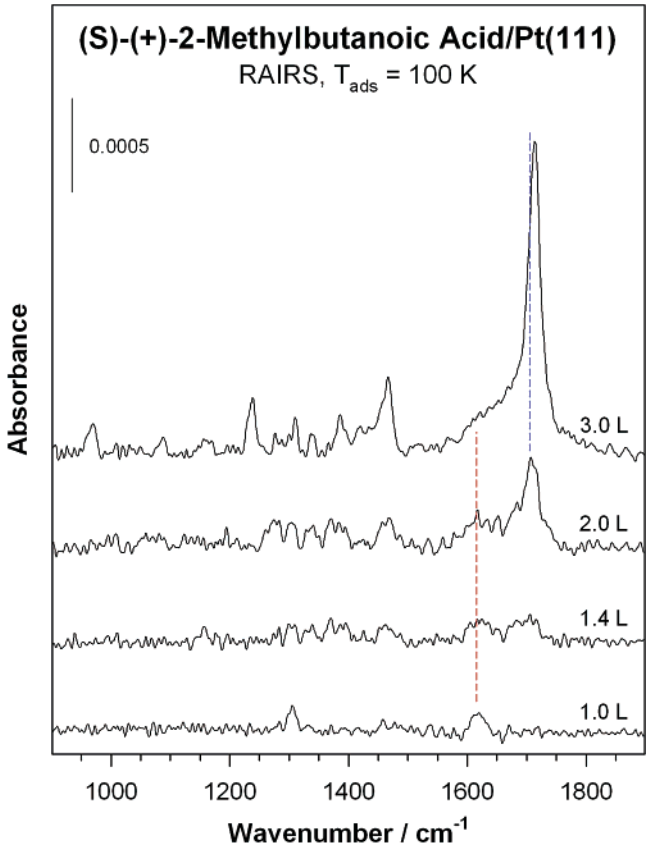

Figure 2. Detail of the RAIRS for the (*S*)-2MBA uptake on Pt(111) at 100 K.

The spectra for the submonolayer coverages of the (*S*)-2MBA at these low temperatures suggest retention of the molecular structure, even though they are still different from those for the multilayer. For one thing, the broad band for the O−H stretching mode around 3100−3500 cm^{-1} is still clearly visible, indicating that no deprotonation has occurred upon adsorption, but has a

(43) Socrates, G. *Infrared Characteristic Group Frequencies: Tables and Charts*, 2nd ed.; Wiley: Chichester, 1994.
(44) Stacchiola, D.; Burkholder, L.; Zheng, T.; Weinert, M.; Tysoe, W. T. *J. Phys. Chem. B* **2005**, *109*, 851.
(45) Kohlrausch, K. W. F.; Koppl, F.; Pongratz, A. *Z. Physik. Chem.* **1933**, *B21*, 242.
(46) NIST Standard Reference Database, http://webbook.nist.gov/chemistry/, Gaithersburg, USA.

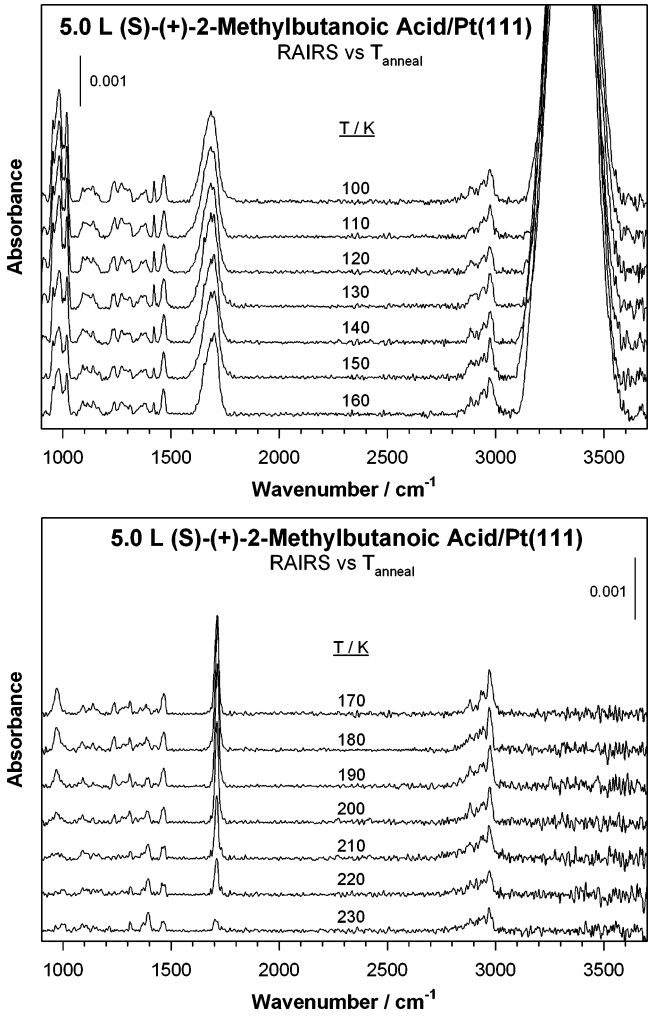

Figure 3. RAIRS data for 5.0 L of (*S*)-2MBA on Pt(111) as a function of annealing temperature. Two transitions become evident from these results, one about 170 K due to multilayer desorption, and a second around 230 K corresponding to a deprotonation step to produce (*S*)-2-methylbutanoate surface species.

distinct shape, with less intensity at the high-frequency end than that in the data for the higher doses. In addition, a number of peaks become quite weak or disappear from the spectra, most likely because of the adoption of a well-defined geometry by the molecule on the surface.[47,48] The two main peaks visible in the low-coverage spectra are those at 1308 and 1620 cm^{-1}, as made more evident in the zoomed data in Figure 2. It is seen there that the latter feature shifts significantly to lower frequencies compared to the value in the free molecule, indicating that adsorption does take place via the carboxylic group. Based on the surface selection rule that applies to RAIRS from metal surfaces,[47,48] it can be concluded that the high intensity of that peak points to a close-to-perpendicular orientation of that group with respect to the surface.

The thermal chemistry of (*S*)-2MBA on Pt(111) was also explored using RAIRS. Figure 3 displays the results obtained for a 5.0 L dose after annealing at different temperatures between 100 and 230 K (in 10 K intervals). Two clear transitions are

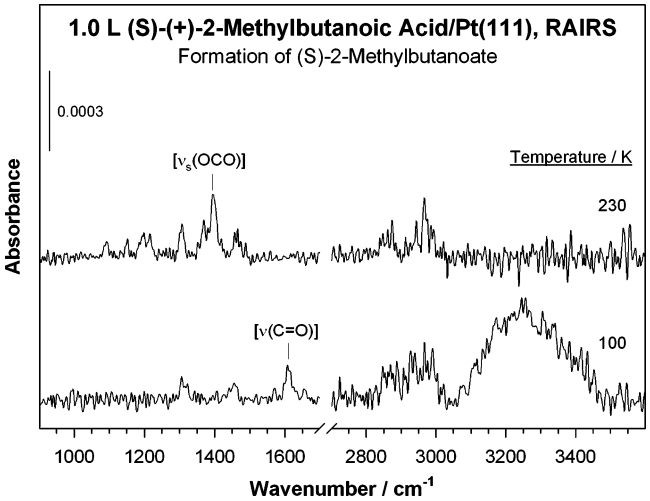

Figure 4. RAIRS evidence for the formation of (*S*)-2-methylbutanoate moieties on the surface. The figure contrasts the spectra obtained for 1.0 L of (*S*)-2MBA adsorbed on the Pt(111) surface at 100 vs 230 K. While the first (bottom trace) clearly displays the peaks corresponding to the C═O (ν(C═O), 1714 cm^{-1}) and hydrogen-bonded OH (ν(OH), 3100−3500 cm^{-1}) stretching modes, the second (top trace) not only lacks those bands but also displays a new peak around 1395 cm^{-1} assignable to the symmetric ν(OCO) mode of carboxylate groups.

observed in those data. The first is seen between 160 and 170 K, where the large and broad feature in the RAIRS data around 3100−3600 cm^{-1} completely disappears. Given that that peak corresponds to the O−H stretching in the carboxylic group of 2-methylbutanoic acid dimers (which are held together by hydrogen bonding), such a change suggests the desorption of all multilayers from the surface. Notice that the peak around 1700 cm^{-1} sharpens up as well, and that the features at 1422, 1018, 983, and 954 cm^{-1}, all associated with modes from methylbutanoic acid dimers, are no longer detectable. On the other hand, the O−H deformation (δ(OH)) peaks at 1385 and 1275 cm^{-1} are still apparent in the spectrum for 170 K, indicating the retention of the molecular nature of the acid at that temperature.

The second thermal transition is seen between 210 and 230 K. Some of the changes observed in that temperature range are somewhat subtle but clearly detectable nevertheless. First of all, the peaks for the O−H deformation vibrational modes, δ-(OH), at 1385 and 1275 cm^{-1}, are no longer visible in the spectra. In addition, the feature for the C═O stretch (ν(C═O)) around 1715 cm^{-1} diminishes significantly in intensity as a new band grows at about 1700 cm^{-1}. These changes are accompanied by the appearance of a new peak at 1394 cm^{-1} assignable to the symmetric stretching of the newly formed carboxylate moiety, as also reported on Pd(111).[44] Finally, there are some additional changes in the relative intensities of the methyl and methylene deformation modes that suggest a different (perhaps more upright) adsorption geometry for the 2-methylbutanoate intermediate that forms on the platinum surface at 230 K. Some of these changes are more evident in the RAIRS data for lower doses (1.0 L) shown in Figure 4. Overall, the RAIRS data indicate multilayer desorption at 170 K and dehydrogenation and carboxylate formation by 230 K. This latter temperature was chosen for the experiments on the formation of chiral suprastructures discussed below.

More information on the thermal chemistry of (*S*)-2MBA on Pt(111) was obtained by temperature programmed desorption

(47) Greenler, R. G. *J. Chem. Phys.* **1966**, *44*, 310.
(48) Zaera, F. Surface Structural Determinations: Optical Methods. In *Encyclopedia of Chemical Physics and Physical Chemistry*; Moore, J. H., Spencer, N. D., Eds.; IOP Publishing Inc.: Philadelphia, 2001; Vol. 2, pp 1563.

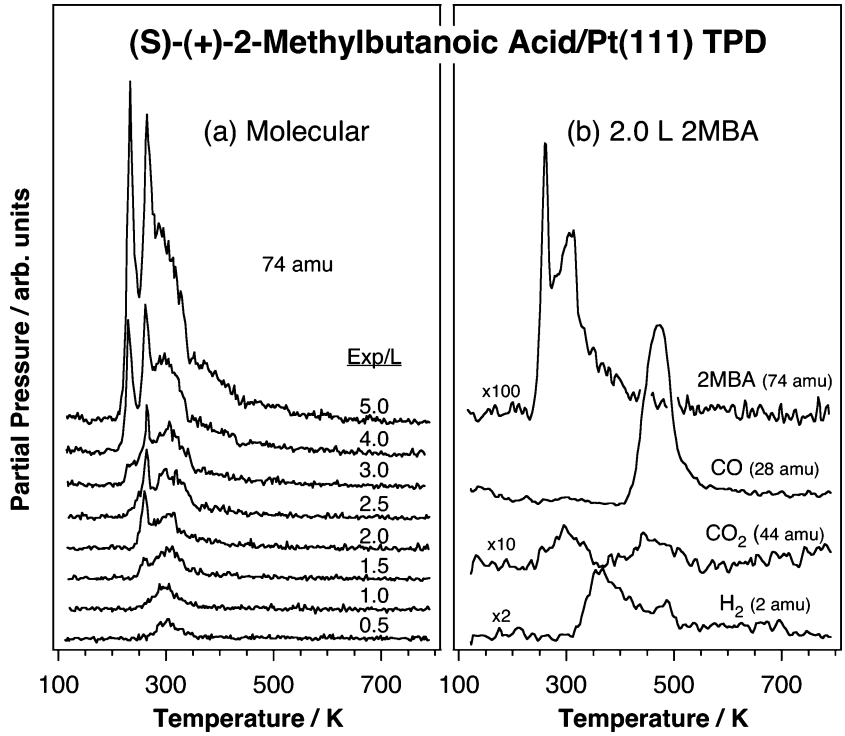

Figure 5. (a, left) Temperature programmed desorption (TPD) data for the molecular evolution of (*S*)-2MBA from Pt(111) as a function of initial dose at 100 K. The signal for 74 amu was used here, but the identity of the adsorbate was corroborated with data from other masses. (b, right) H_2, CO_2, CO, and molecular TPD from 2.0 L of (*S*)-2MBA adsorbed on Pt(111) at 100 K. Besides molecular desorption, only the production of hydrogen, carbon monoxide, and carbon dioxide is seen in this case. Molecular desorption displays three regimes, which fill up sequentially as a function of exposure.

(TPD). The left panel of Figure 5 displays the traces obtained for (*S*)-2MBA molecular desorption as a function of exposure after adsorption on Pt(111) at 100 K. The signal for 74 amu was used here, but the identity of the desorbing species was confirmed by also recording the data for 57, 87, and 102 amu. Three states populate sequentially with increasing exposures: (1) a feature around 300 K, seen even at the lowest exposures, which saturates by 1.5 L; (2) a sharp monolayer desorption peak, seen first at 260 K in the 1.5 L trace and about 265 K by 5.0 L; and (3) a multilayer region around 230 K starting at 2.5 L. Notice that the exposure onset of this latter state coincides with the development of the additional high-frequency signal for the ν(OH) vibrational mode of the (*S*)-2MBA dimers in the uptake RAIRS data in Figure 1. Also, it is at that temperature that the dehydrogenation of adsorbed (*S*)-2MBA to the (*S*)-2-methylbutanoate species is seen in Figures 3 and 4.

The right panel of Figure 5 shows the TPD traces obtained for the decomposition products that desorb during thermal activation of 2.0 L of (*S*)-2MBA chemisorbed on Pt(111). Only hydrogen, carbon monoxide, and carbon dioxide were detected in these experiments. Other species searched for but not seen include 2-methyl-1-butanol (41, 70, 88 amu), propanoic acid (45, 57, 74 amu), and propenoic acid (45, 55, 72 amu). Signals were detected for 41, 45, 55, and 57 amu, but those followed closely the shape and relative intensities expected from molecular (*S*)-2MBA. In Figure 5b it is seen that hydrogen desorbs in two regimes, around 365 and 487 K. The first is clearly desorption limited and includes not only the hydrogen from deprotonation of the carboxylic group but also subsequent extensive dehydrogenation of the aliphatic chain. In terms of the CO_2 TPD trace, some decarboxylation is seen already at 305 K. That is likely to lead to the formation of 2-butyl surface groups, which would be expected to undergo β-hydride elimination immediately to produce adsorbed 2-butene.[49−51] Additional carbon dioxide desorbs at 470 K, but that is accompanied by significant H_2 and CO production and, therefore, indicates more extensive and nonselective decomposition.

3.2. Coadsorption of (*S*)-(+)-2-Methylbutanoic Acid and Propylene Oxide. The next step in our research was to test the potential enantioselectivity of the (*S*)-2-methylbutanoate layers on Pt(111) by using enantiopure propylene oxide (PO) as a probe molecule. This type of work has proven successful before in studies with 2-butoxide layers on Pt(111)[36] and with 2-butoxide[35] and 2-methylbutanoate[44] on Pd(111). In the present case, the success of the experiments relied on the following facts: (1) that (*S*)-2-methylbutanoate species can be prepared cleanly on Pt(111) upon heating adsorbed (*S*)-2MBA to temperatures around 230 K; (2) that PO desorbs at detectably higher temperatures from the first monolayer than from multilayers; and (3) that the PO monolayer also shows clear differences in the IR spectra compared to those from the multilayer, in particular a shift in frequency of the ring deformation mode, δ_{oop}(ring), from 830 to 822 cm^{-1}.

Figures 6 and 7 show results from experiments designed to measure surface enantioselectivity using TPD. In these experiments, defined amounts of enantiopure (*S*)-2MBA were first adsorbed on a Pt(111) surface at 100 K and annealed to 230 K to produce the appropriate layers of (*S*)-2-methylbutanoate surface species. Those samples were subsequently saturated with 2.0 L of enantiopure (*R*)- or (*S*)-PO at 100 K, after which TPD data for the PO desorption were recorded. Figure 6 reports the

(49) Lee, I.; Zaera, F. *J. Phys. Chem. B* **2005**, *109*, 2745.
(50) Zaera, F. *Catal. Lett.* **2003**, *91*, 1.
(51) Zaera, F. *Acc. Chem. Res.* **1992**, *25*, 260.

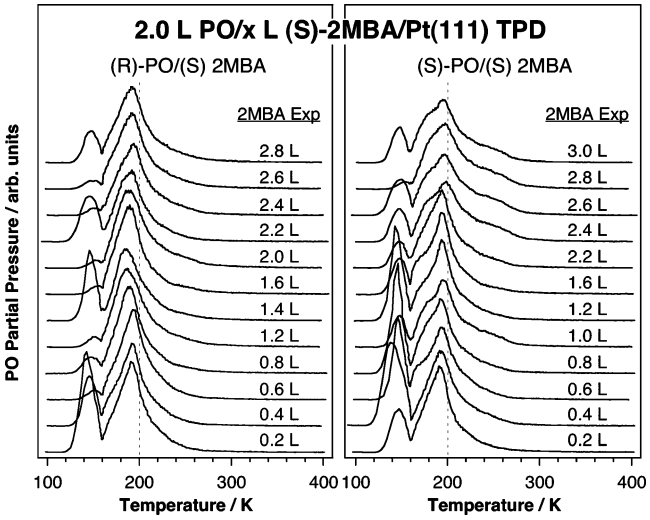

Figure 6. Propylene oxide (PO, 58 amu) TPD data from PO titration experiments of 2-methylbutanoate chiral layers adsorbed on Pt(111) as a function of the (*S*)-2MBA initial exposure used to prepare the butanoate layers (by dosing at 100 K and annealing at 230 K). In these experiments 2.0 L of the PO were dosed at 100 K after the formation of the chiral templated surface. The left panel shows the data for titrations using (*R*)-PO, while the right displays the equivalent results with (*S*)-PO. Both the peaks intensities and the peak positions are quite different in the (*R*)-PO/(*S*)-2MBA/Pt(111) (*RS*) vs (*S*)-PO/(*S*)-2MBA/Pt(111) (*SS*) cases, and also evolve differently as the initial methylbutanoate coverage is increased.

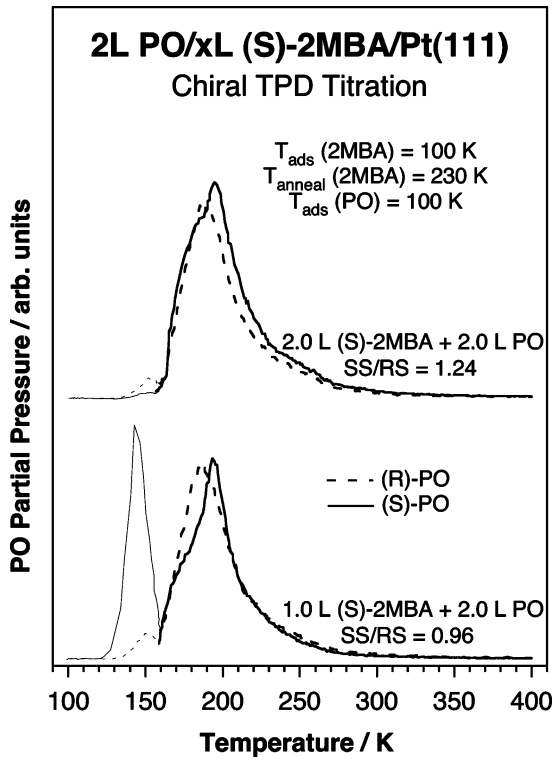

Figure 7. Comparison of (*R*)- vs (*S*)-PO TPD data from titration experiments of the 2-methylbutanoate chiral layers using propylene oxide. Specific examples were selected here, for 1.0 L (bottom traces) and 2.0 L (top traces) of (*S*)-2MBA, to highlight the differences seen between the titrations with the two PO enantiomers. Indeed, while the yields for the two PO enantiomers are similar in the 1.0 L (*S*)-2MBA case, they are quite different for the 2.0 L of (*S*)-2MBA example, where the *SS*/*RS* ratio reaches a value of 1.24. In addition, the peak shapes are quite different with (*R*)- vs (*S*)-PO, indicating different energetics of adsorption.

respective sets of TPD traces for the (*R*)-PO/(*S*)-2MBA/Pt(111) (*RS*, left) and (*S*)-PO/(*S*)-2MBA/Pt(111) (*SS*, right) combinations. Clear differences are seen between the two sets in terms of peak shapes, peak intensities, and developments with increasing (*S*)-2MBA exposure, as shown more clearly for the cases of 1.0 and 2.0 L of (*S*)-2MBA in Figure 7. In particular, a higher monolayer PO desorption yield is seen in the case of 2.0 L of (*S*)-2MBA with (*S*)-PO (solid traces) than with (*R*)-PO (dashed lines). Indeed, the PO TPD yield ratio for the (*S*)-PO/(*S*)-2MBA/Pt(111) versus (*R*)-PO/(*S*)-2MBA/Pt(111) systems (SS/RS for short) amounts to 1.24 after the 2.0 L (*S*)-2MBA dose, in contrast with the 0.96 value seen after the 1.0 L dose. This indicates a preference for adsorption of the same type of enantiomer of the propylene oxide on the chiral methylbutanoate layer after the higher exposure. A full analysis of the TPD traces for the dependence of this enantioselectivity on the (*S*)-2MBA dose provided in Figure 6 resulted in the data shown in Figure 8. There, it is clear that this chiral effect is operative on the (*S*)-2-methylbutanoate layers obtained after (*S*)-2MBA doses between 1.8 and 2.4 L. It should also be pointed out that the energetics of the PO desorption are quite different with (*R*)- versus (*S*)-PO. This is indicated by the different shapes of the monolayer PO TPD peaks in Figures 6 and 7: the data for (*R*)-PO/(*S*)-2MBA/Pt(111) display one broad feature around 188 K, whereas the (*S*)-PO/(*S*)-2MBA/Pt(111) case results in two overlapping features at 175 and 195 K. This difference was observed over the whole range of (*S*)-2MBA exposures studied here. Also, the differences in both peak shape and peak position are large enough to be well outside the experimental errors of the TPD technique.

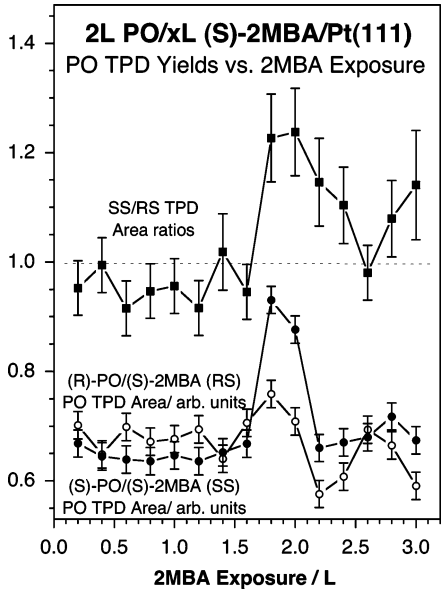

Figure 8. PO TPD yields from chiral titrations of (*S*)-2-methylbutanoate layers on Pt(111) with 2.0 L of either (*S*)-PO (●) or (*R*)-PO (○) as a function of (*S*)-2MBA initial dose. Also shown are the ratios of the yields for the *SS* vs *RS* combinations. The clear deviation from unity seen between 1.8 and 2.4 L of (*S*)-2MBA attest to the enantioselectivity of the methylbutanoate layers toward PO adsorption in that coverage range.

Finally, Figure 9 provides further evidence from RAIRS experiments corroborating the enantioselectivity of the adsorption of PO on (*S*)-2-methylbutanoate chiral surface layers. In this case, again, either 1.0 (Figure 9a) or 2.0 (Figure 9b) L of (*S*)-2MBA were first adsorbed on the Pt(111) surface at 100 K and annealed at 230 K to produce the (*S*)-2-methylbutanoate layers. Afterward, 2.0 L of either (*S*)- (top traces) or (*R*)- (bottom

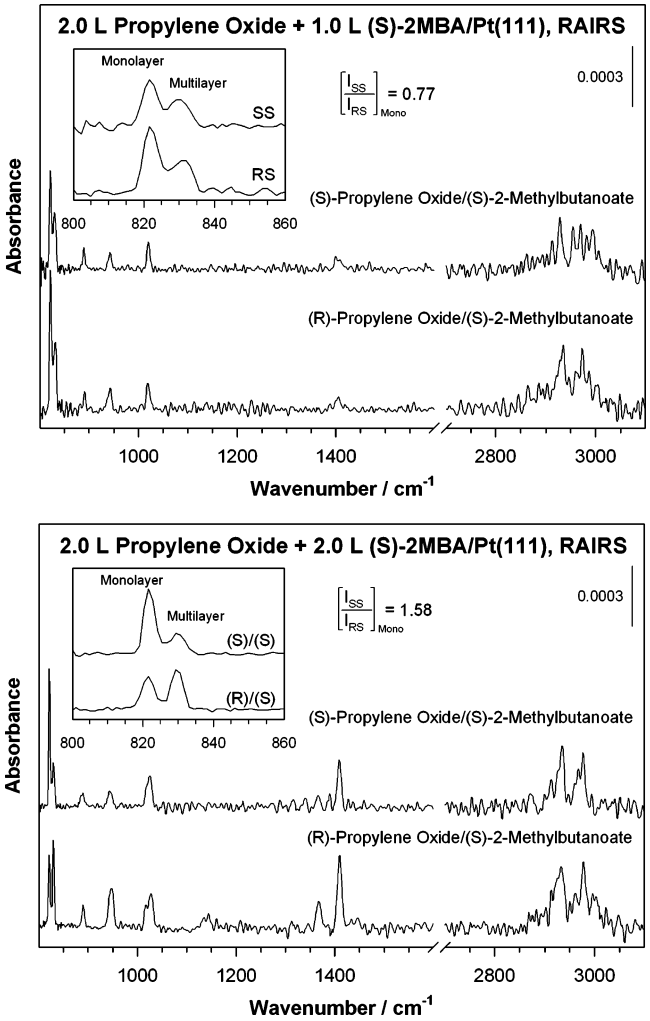

Figure 9. RAIRS from Pt(111) surfaces sequentially treated with (*S*)-2MBA and PO in the same way as described in Figure 6. Panels (a, top) and (b, bottom) correspond to (*S*)-2MBA doses of 1.0 and 2.0 L, respectively, while the bottom and top traces in each correspond to 2.0 L doses of (*R*)- and (*S*)-PO, respectively. A number of differences are seen between the two spectra in each panel. Specifically, the intensity of the peak at 822 cm^{-1}, due to the ring deformation mode in the PO monolayer (shown in detail in the insets), is about 77% as large in the *SS* combination compared to the *RS* pair for the 1.0 L (*S*)-2MBA dose but 158% as large after a 2.0 L (*S*)-2MBA dose.

traces) PO were dosed at 100 K. The differences in monolayer PO adsorption were identified mainly by following the intensity of the vibrational band associated with its ring deformation, δ_{oop}(ring), at 822 cm^{-1} (data enlarged in the inset); the peak at 830 cm^{-1} corresponds to the same mode for the PO condensed in multilayers.[35,36] Large differences are seen in the intensity of that signal: while a ratio for the (*S*)-PO/(*S*)-2MBA/Pt(111) pair against the (*R*)-PO/(*S*)-2MBA/Pt(111) (I_{SS}/I_{RS}) of only 0.77 was measured for the 1.0 L (*S*)-2MBA dose (Figure 9a), a value of 1.58 is obtained for the 2.0 L case (Figure 9b). Interestingly, this switch is due not only to an increase in the absolute intensity of the peak in the *SS* case but also to a decrease of the same feature in the *RS* pair, in which case the remaining PO is detected in the multilayer. The behavior of the peaks from the $\rho(CH_2)$, $\rho(CH_3)$, and $\omega(CH_3)$ propylene oxide vibrational modes at 890 (906), 942 (954), and 1020 (1030) cm^{-1} in the monolayer (multilayer) is consistent with that of the ring deformation. Again, it is clear from the RAIRS data that the (*S*)-2-methylbutanoate layer can provide more adsorption sites for the propylene oxide probe with the same chirality. Note, however, that with RAIRS it is not easy to quantify this effect because of the additional dependence of the vibrational signal intensities on molecular orientation.[47,48]

4. Discussion

As mentioned in the Introduction, it is possible to impart enantioselectivity to achiral surfaces by adsorbing enantiopure modifiers. Two prevailing mechanisms have been proposed for this, one where the chiral molecule forms an individual complex with the reactant to force a particular adsorption geometry on the surface,[18,19] and another where it is the collective arrangement of the chiral modifiers on the surface that allows the formation of enantioselective surface sites.[30] It is implicitly assumed that the first mechanism requires relatively elaborated molecules such as cinchonas, while the second is more likely when simpler structures are involved. However, it is still not known what parameters determine the effectiveness of the chiral modifiers in either case or what makes one mechanism dominate over the other.

Regardless of the microscopic details, however, what has been clearly shown already is that single-crystal surfaces templated with chiral adsorbates can display enantioselectivity toward the adsorption of enantiopure chiral molecules.[35,36,44,52] The data available so far suggest that this may in fact be a fairly general phenomenon. Indeed, Tysoe et al. have detected such a behavior for a number of alcohols, organic acids, and amino acids on Pd(111),[35,37,44] and our past work with 2-butanol on Pt(111) has indicated that the same may apply to other surfaces.[36] On the other hand, Tysoe's studies also identified some notable exceptions: no enantioselectivity was seen on Pd(111) with 2-methylbutanoic acid, valine, or leucine.[37] To explain this observation, and basing their discussion on the possible formation of chiral surface suprastructures in the systems they studied, the Tysoe group advanced the hypothesis that chiral templating perhaps requires two anchoring points for the molecule on the surface.[53] It was argued that otherwise the free rotation around the single pivotal adsorption point could wash out any surface chirality.

The results reported here bring into question the validity of that hypothesis. Although the enantioselectivity observed in our study for (*R*)- vs (*S*)-propylene oxide adsorption is not as high as that seen in other cases, it is clearly detectable, and argues for other factors playing a role in defining chirality on the surface. A more systematic investigation varying the templating and probe molecules as well as the nature and structure of the surface is needed to better determine the parameters that define the surface enantioselectivity. Nevertheless, the data shown above do provide some clues on additional factors to be taken into consideration when describing this chiral surface chemistry. In particular, it is to be noted that in all previously reported chiral titration experiments enantioselectivity was identified by variations in the extent of adsorption of the chiral probe, that is, by the differences in yield in the TPD experiments with (*R*)- versus (*S*)-propylene oxide adsorbed on specific chirally templated surfaces. This is because, except for some minor shifts

(52) Raval, R. *J. Phys.: Condens. Matter* **2002**, *14*, 4119.
(53) Romá, F.; Stacchiola, D.; Tysoe, W. T.; Zgrablich, G. *Physica A* **2004**, *338*, 493.

in peak position seen in the 2-butanol/Pt(111) case,[36] no detectable differences in the energetics of propylene oxide adsorption had been observed in the homochiral versus heterochiral pairs (that is, in the *RR* or *SS* versus *RS* or *SR* combinations).

That is clearly not the case here. Specifically, the TPD data in Figures 6 and 7 show quite different desorption profiles from (*R*)- versus (*S*)-propylene oxide on Pt(111) precovered with (*S*)-2-methylbutanoate layers. While the traces for (*R*)-PO display one single broad feature around 188 K, in the (*S*)-PO case a main peak is seen at 195 K (together with a low-temperature shoulder about 175 K). Therefore, it appears that most of the propylene oxide in the homochiral *SS* system adsorbs more strongly than in the *RS* case. A rough estimate of activation energies using a Redhead analysis[54] indicates an adsorption energy difference of about 0.5 kcal/mol, or approximately 4% of the total energy barrier. This difference, coincidentally, is comparable to that reported previously for the adsorption of PO and other small molecules on intrinsically chiral surfaces, in which case the effect was ascribed to interactions with the chiral surface kinks.[55,56] It could be suggested that small energy differences may be induced in chiral surfaces by the immediate chirally templated surroundings. On the other hand, it is not easy to identify here either of the two energy states seen in the TPD for the *SS* case with specific adsorption sites, or to determine which one is responsible for the increase in enantioselectivity seen around 2.0 L (*S*)-2MBA doses, because no clear trends were observed in the shape of the TPD traces as a function of (*S*)-2MBA exposure (Figure 6). This is coupled with the fact that the absolute PO TPD yields do not vary much with the amount of (*S*)-2MBA initially dosed on the surface. Indeed, the PO yields reported in Figure 8 are almost constant in the 0.2−1.6 L (*S*)-2MBA dose range, and also similar after 2.2 L.

This brings up another interesting observation from the results of the present study: that the chiral templating effect in the (*S*)-2-methylbutanoate/Pt(111) system is in fact not strongly dependent on the number of adsorption sites available for the (*R*)- or (*S*)-PO chiral probe. This is because varying the initial dose of (*S*)-2MBA on the Pt(111) does not affect the surface area covered by the (*S*)-2-methylbutanoate layer produced after annealing at 230 K. Instead, that appears to change the nature of that layer instead. It is inferred here that it is the changes in either the geometry of the (*S*)-2-methylbutanoate or the way that those moieties pack on the surface that is affected by the initial (*S*)-2MBA dose. Several clues point to that fact. Specifically, three different molecular states were identified in the TPD uptake data in Figure 5, from which the onsets of the desorption of the second (265 K) and third (230 K), after (*S*)-2MBA doses of approximately 1.5 and 2.5 L, roughly define the range where enantioselectivity is seen afterward (Figure 8). The same can be said for the RAIRS uptake spectra in Figure 1. There, a first transition around 1.6 L is indicated by the growth or sharpening of many of the vibrational features, in particular the ν(C═O) peak about 1705 cm^{-1}. The low-exposure spectra only show two prominent peaks at 1308 and 1620 cm^{-1}, suggesting a carboxylic group standing up but a flat hydrocarbon chain (since those modes are not seen in the data). In fact, even the latter modes are weak in the spectra of low (*S*)-2MBA doses with coadsorbed PO, so the whole molecule may in those cases be laying down on the surface. Perhaps exposures above 1.5 L force a change in geometry to improve packing. A second change is seen above 2.6 L due to multilayer condensation.

Further support for our idea comes from the RAIRS data in Figure 9. Although the majority of the peaks in that figure are ascribed to propylene oxide, the signal around 1410 cm^{-1} is likely to originate mostly from the 2-methylbutanoate surface species (although there may be some interference with the methylene scissoring mode in propylene oxide).[36] Notice that this feature is slightly blue-shifted from the position at which it is observed in the spectra for the pure 2-methylbutanoate layer (Figure 4), perhaps because of changes induced by the coadsorbed propylene oxide. This points to one important fact already indicated in the study of the 2-butanol/Pt(111) system: that there are synergies between the chiral templating layers and the propylene oxide chiral probe.[36] More relevant here, the 1410 cm^{-1} peak is much more intense after the 2.0 L (*S*)-2MBA dose than in the 1.0 L (*S*)-2MBA case (compare the spectra in Figure 9a vs 9b). This is true for both *RS* and *SS* pairs. It seems that the higher coverages obtained with the 2.0 L (*S*)-2MBA dose require closer packing on the surface and that that pushes the adsorbates into a geometry with the carboxylic group standing up on the surface. In the case of the 1.0 L dose, the weak intensity of that IR feature suggests a flatter geometry.

In summary, there is evidence in this (*S*)-2-methylbutanoate/Pt(111) system for both strong one-to-one interactions between the modifier and the probe and the formation of chiral suprastructures on the surface. It could be argued that this makes the present a good example of an intermediate case between the two proposed chiral-bestowing mechanisms on achiral surfaces by chiral modifiers. However, it does appear that it is the long-range ordering that induces the chiral behavior observed. Although stronger interactions between modifier and probe are seen in the *SS* pair compared to the *RS* case, those are operative over the whole range of initial (*S*)-2MBA doses, beyond where enantioselectivity is observed. In addition, the approximately constant yields seen in the PO TPD, as reported in Figure 8, strongly suggest that there must be a change in adsorption geometry or surface packing of the (*S*)-2-methylbutanoate species with increasing (*S*)-2MBA initial dose. This appears to be the only way to explain both the constant surface coverage of empty sites for PO adsorption and the change in enantioselectivity reported above as a function of (*S*)-2MBA exposure. The RAIRS data support this conclusion. Nevertheless, it is quite possible that the energetic differences between the *RS* vs *SS* pairs either induce or are a consequence of different packings of the (*S*)-2-methylbutanoate fragments on the Pt(111) surface. In fact, since both sets of experiments start with the same (*S*)-2-methylbutanoate/Pt(111), it is most likely that the propylene oxide is at least partly responsible for the differences in the behavior of the surface in the two cases. Perhaps the stronger (*S*)-PO/(*S*)-2-methylbutanoate interactions lead to a more extensive surface rearrangement of the adsorbates there. It is suggested here that the templated surfaces cannot just be viewed as static, but that the chiral adsorption sites exposed by the modifier suprastructures may be at least in part be tailored during the subsequent adsorption of the chiral probe (or

(54) Redhead, P. A. *Vacuum* **1962**, *12*, 203.
(55) Hazen, R. M.; Sholl, D. S. *Nat. Mater.* **2003**, *2*, 367.
(56) Horvath, J. D.; Koritnik, A.; Kamakoti, P.; Sholl, D. S.; Gellman, A. J. *J. Am. Chem. Soc.* **2004**, *126*, 14988.

reactant). Monte Carlo modeling is currently under way to try to test all these hypothesis and conclusions.

5. Conclusions

Temperature programmed desorption and reflection adsorption infrared spectroscopies were used to characterize the adsorption, surface chemistry, and chiral-bestowing ability of 2-methylbutanoic acid on Pt(111). At low temperatures 2-methylbutanoic acid adsorbs molecularly by bonding to the surface through its carboxylic group. At higher temperatures molecular desorption takes place in two stages corresponding to multilayer dimers and the monolayer, and deprotonation occurs at even higher temperatures, about 230 K, and leads to 2-methylbutanoate formation. Some decarbonylation is possible around 300 K, presumably causing the sequential formation of 2-butyl and 2-butene adsorbed intermediates, and more extensive decomposition into CO, CO_2, H_2, and surface carbon takes place above 470 K.

The enantiopure (*S*)-2-methylbutanoate layers that form on Pt(111) upon thermal activation of adsorbed (*S*)-(+)-2-methylbutanoic acid appear to form chiral superstructures on the surface, as manifested by the preferential adsorption of propylene oxide with the same chirality as the underlying layer. Specifically, an approximately 25% increase in propylene oxide uptake is seen when using the (*S*)-PO instead of the (*R*)-PO enantiomer in the range between about 1.8 and 2.4 L of (*S*)-(+)-2-methylbutanoic acid exposure. Most of the (*S*)-propylene oxide adsorbs more strongly than the (*R*) counterpart on these (*S*)-2-methylbutanoate layers, but this is true in all instances, even when no enantioselectivity is observed, and therefore must not be the primary cause for the resulting surface chirality. Instead, indirect TPD and RAIRS evidence points to changes in 2-methylbutanoate adsorption geometries, and perhaps to different 2-methylbutanoate surface packing induced by (*R*)- versus (*S*)-propylene oxide.

Acknowledgment. Funding for this research was provided by a grant from the U.S. Department of Energy.

JA061654W